Template Syntheses of Polypyrrole Nanowires and CdS Nanoparticles in Porous Polymer Monoliths

Bret J. S. Johnson, Johanna H. Wolf, Andrew S. Zalusky, and Marc A. Hillmyer*

Department of Chemistry, University of Minnesota, 207 Pleasant Street SE, Minneapolis, Minnesota 55455-0431

Received October 14, 2003. Revised Manuscript Received March 11, 2004

Template synthesis is a powerful method for the preparation of nanoscale materials with specific size and shape. We describe the template synthesis of polypyrrole nanowires and CdS nanoparticles within monolithic nanoporous polymer templates prepared from ordered block copolymer precursors. SAXS measurements confirmed retention of the host structure after growth of the nanomaterials within the pores of the template. SEM and TEM were used for direct visualization of the size and shape of the templated materials both in the monolith as well as after removal of the template through dissolution. The size of the templated nanomaterials matched that of the template pores and was modifiable by using templates containing different pore dimensions. For the case of CdS nanoparticles, WAXS was also used to verify particle size and crystal structure. In an effort to impregnate the nanoporous monoliths with CdS particles smaller than the pore dimensions of the template, a synthetic protocol utilizing a capping agent was employed. These particles were shown to exhibit a quantum size effect by DR−UV−Vis.

Introduction

The ability to control the shape, size, and morphology of materials on the nanometer length scale is an important factor for defining properties such as the electronic band gap[1] and conductivity or light emission efficiency.[2] This control can be achieved using templates of the appropriate size scale and topology.[3,4] These nanotemplate methods involve restricted growth within a porous host structure and thus rely on the shape of the pores to determine the final morphology of the material. Porous inorganic frameworks have been used as templates for the synthesis of nanostructured materials,[5−10] and a particularly versatile method for template syntheses has been developed by Martin and co-workers using porous polycarbonate films. Nanowires of varying composition, from gold to poly(3-methyl thiophene), have been synthesized using this methodology.[11−13] Several other groups have also used the template synthesis approach to produce conducting polymer[14−17] or metallic[18] nanowires from porous polymer templates. Composite structures containing nanomaterials in anisotropic configurations can be prepared from specific templates. A significant portion of the work with polymeric hosts has focused on producing ordered nanoporous thin films that can be used as templates for nanoparticles[19,20] or masks for patterning surfaces.[21,22] The use of monolithic nanoporous polymer frameworks can lead to nanomaterials with larger aspect ratios than those obtained via nanoporous thin films.

We have previously described the preparation of monolithic nanoporous polystyrene (PS) and its hydrogenated counterpart, polycyclohexylethylene (PCHE), from ordered block copolymer precursors.[23−26] These

* To whom correspondence should be addressed. E-mail: hillmyer@chem.umn.edu.

(1) Alivisatos, A. P. *Science* **1996**, *271*, 933−937.
(2) Kim, J.; Sohn, D.; Sung, Y.; Kim, E.-R. *Synth. Met.* **2003**, *132*, 309−313. Also see: Huang, J.; Kaner, R. B. *J. Am. Chem. Soc.* **2004**, *126*, 851.
(3) Shim, M.; Guyot-Sionnest, P. *J. Am. Chem. Soc.* **2001**, *123*, 11651−11654.
(4) Yang, H.; Ozin, G. A.; Kresge, C. T. *Adv. Mater.* **1998**, *10*, 883−887.
(5) Zelenski, C. M.; Hornyak, G. L.; Dorhout, P. K. *Nanostruct. Mater.* **1997**, *9*, 173−176.
(6) Hulteen, J. C.; Martin, C. R. *J. Mater. Chem.* **1997**, *7*, 1075−1087.
(7) Johnson, S. A.; Brigham, E. S.; Ollivier, P. J.; Mallouk, T. E. *Chem. Mater.* **1997**, *9*, 2448−2458.
(8) Zhu, K.; Yue, B.; Zhou, W.; He, H. *Chem. Commun.* **2003**, 98−99.
(9) Yang, H.; Shi, Q.; Liu, X.; Xie, S.; Jiang, D.; Zhang, F.; Yu, C.; Tu, B.; Zhao, D. *Chem. Commun.* **2002**, 2842−2843.
(10) Kang, M.; Yi, S. H.; Lee, H. I.; Yie, J. E.; Kim, J. M. *Chem. Commun.* **2002**, 1944−1945.
(11) Wirtz, M.; Martin, C. R. *Adv. Mater.* **2003**, *15*, 455−458.
(12) Cai, Z.; Lei, J.; Liang, W.; Menon, V.; Martin, C. R. *Chem. Mater.* **1991**, *3*, 960−967.
(13) Menon, V. P.; Lei, J. L.; Martin, C. R. *Chem. Mater.* **1996**, *8*, 2382−2390.
(14) Mativetsky, J. M.; Datars, W. R. *Physica B* **2002**, *324*, 191−204.
(15) Li, X.; Zhang, X.; Li, H. *J. Appl. Polym. Sci.* **2001**, *81*, 3002−3007.
(16) Demoustier-Champagne, S.; Ferain, E.; Jerome, C.; Jerome, R.; Legras, R. *Eur. Polym. J.* **1998**, *34*, 1767−1774.
(17) Schonenberger, C.; Zande, B. M. I. v. d.; Fokkink, L. G. H.; Henny, M.; Schmid, C.; Kruger, M.; Bachtold, A.; Huber, R.; Birk, H.; Staufer, U. *J. Phys. Chem. B* **1997**, *101*, 5497−5505.
(18) Demoustier-Champagne, S.; Delvaux, M. *Mater. Sci. Eng. C* **2001**, *15*, 269−271.
(19) Hashimoto, T.; Tsutsumi, K.; Fuanaki, Y. *Langmuir* **1997**, *13*, 6869−6872.
(20) Misner, M. J.; Skaff, H.; Emrick, T.; Russell, T. P. *Adv. Mater.* **2003**, *15*, 221−224.
(21) Mansky, P.; Harrison, C. K.; Chaikin, P. M.; Register, R. A.; Yao, N. *Appl. Phys. Lett.* **1996**, *68*, 2586−2588.
(22) Black, C. T.; Guarini, K. W.; Milkove, K. R.; Baker, S. M.; Russell, T. P.; Tuominen, M. T. *Appl. Phys. Lett.* **2001**, *79*, 409−411.
(23) Zalusky, A. S.; Olayo-Valles, R.; Taylor, C. J.; Hillmyer, M. A. *J. Am. Chem. Soc.* **2001**, *123*, 1519−1520.

10.1021/cm0350075 CCC: $27.50
Published on Web 06/25/2004

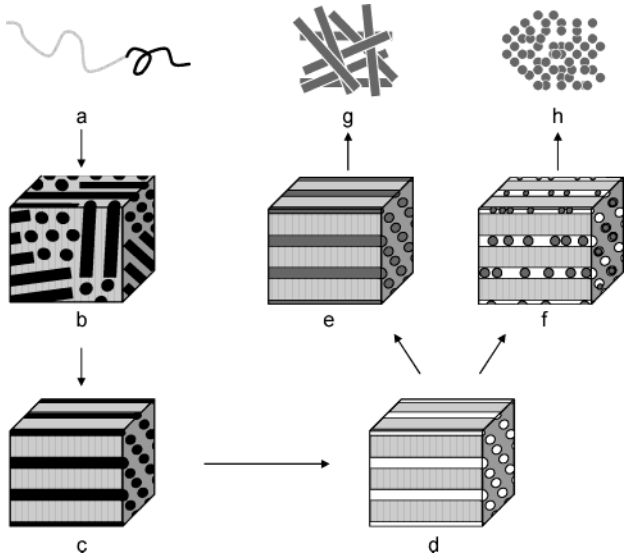

Figure 1. Pathway to nanostructured materials: (a) diblock copolymer, (b) polygranular cylindrical morphology, (c) macroscopically aligned cylindrical morphology achieved by flow orientation, (d) removal of minor component to yield nanoporous template, (e) and (f) preparation of nanowires and nanoparticles within the template, respectively, and (g) and (h) removal of template to obtain nanostructured materials.

materials are ideal as nanomaterial templates for several reasons. They contain 10^{11} pores per cm^2 that are aligned along a preferred direction and exhibit narrow size distributions. Furthermore, the frameworks are stable to a variety of chemical environments and easily removed by simple dissolution. The pores are arranged in ordered hexagonal arrays and pore sizes can be systematically tuned by controlling the molecular weight of the copolymer precursor. Given the monolithic nature of these templates (i.e., not thin films), materials grown inside can in principle exhibit unusually large aspect ratios. The pore walls are lined with accessible hydroxyl groups that may be exploited for subsequent functionalization. A schematic showing the preparation of nanoporous templates from ordered block copolymers along with the synthesis of nanomaterials within the resulting templates is shown in Figure 1.

In this paper we describe two syntheses using monolithic nanoporous polymer templates, a conducting polymer, polypyrrole (PPY), and an inorganic semiconductor, CdS. Polypyrrole is one of the most stable conducting polymers and is readily deposited into useful forms despite its insolubility and infusibility.[27] Because of the relatively high vapor pressure of the pyrrole monomer, PPY is synthesized by vapor-phase polymerization in the presence of an appropriate oxidant (e.g., $FeCl_3$).[2] Vapor-phase polymerization is particularly attractive using small-pore templates where rapid solution-phase polymerizations may block the pore ends, prohibiting polymer growth further within the template. Here we show that PPY nanowires with a variety of diameters can be successfully templated within nanoporous PCHE monoliths.

CdS, easily synthesized by the reaction of Cd^{2+} with a source of S^{2-}, is one of the most studied II−IV semiconductors and it is often used as a model system when studying nanocrystals or semiconductors.[28] In this work, reagents were adsorbed in the nanoporous material in two steps to form CdS nanoparticles within the nanostructured templates. We demonstrate that CdS particles of varying diameter can be synthesized within nanoporous PS hosts where the size of the particles is dependent on the pore dimensions of the host. The synthesis was also modified to obtain particles within the nanoporous monolith that were smaller than the template pore dimensions, and these particles showed a quantum size effect.

Experimental Section

General Methods. All solution ^1H NMR and ^{13}C NMR spectra were obtained using a Varian 300 VI spectrometer. Polymer samples were dissolved in deuterated chloroform (Cambridge) at approximate concentrations of 1.0 wt %. The $^{13}C\{^1H\}$ MAS NMR spectra were collected on a 400 MHz Chemagnetics spectrometer at a spin rate of 5 kHz and referenced to hexamethylbenzene. The size exclusion chromatography (SEC) experiments were performed on a Hewlett-Packard 1100 series liquid chromatograph equipped with Jordi polydivinylbenzene columns with pore sizes of 10000, 1000, and 500 Å and a Hewlett-Packard 1047A differential refractometer. The experiments were carried out at 40 °C with THF as the mobile phase at a flow rate of 1 mL/min. Infrared (IR) spectroscopy was performed using a Nicolet Magna-IR spectrometer. Samples were prepared as thin films cast from solution onto polished sodium chloride salt plates or were pressed into potassium bromide pellets. The spectra were an average of 32 scans. UV analyses were performed on a Spectronic Instruments Genesys 5 spectrophotometer in THF at approximate concentrations of 1 mg/mL. Diffuse reflectance UV−Vis absorption spectra were collected on a Hewlett-Packard 8452A diode array UV−visible spectrophotometer with a Labsphere RSA-HP-84 reflectance spectroscopy accessory. Reflectance data were converted to $f(R_\infty)$ using the Kubelka−Munk equation. WAXS was performed on a Siemens D5005 X-ray diffractometer with Cu Kα radiation. SAXS measurements were taken at the University of Minnesota on a home-built line. Cu Kα X-rays with a wavelength of 1.542 Å were generated through a Rigaku RU-200BVH rotating anode X-ray machine fitted with a 0.2×2 mm^2 microfocus cathode and Franks mirror optics. The sample was mounted in a brass block (temperature controlled by electrical heating and water cooling) in a vacuum-sealed chamber. Two-dimensional (2D) diffraction patterns were recorded using a Siemens multiwire detector and were corrected for detector response before analysis. The 2D scattering patterns were azimuthally integrated to a 1D plot of intensity versus $q = 4\pi\lambda^{-1}\sin(\theta/2)$, where λ and θ are the radiation wavelength and scattering angle, respectively. The detector distance was 230 cm for most samples, and data were typically collected for a 10−15 min period for diblock copolymer samples and a 0.5−1 min period for porous samples. The samples were examined with the X-ray beam probing the samples perpendicular to the preferred direction of the PLA morphology or cylindrical pores. SEM analysis was performed on an Hitachi S-900 FE-SEM using accelerating voltages of 3−5 keV. SEM samples were prepared by cutting the nanoporous monoliths with a razor blade and mounting them onto brass shims with colloidal graphite (Ted Pella). The samples were sputter-coated with 2−3 nm of platinum (estimated from a calculated deposition rate and experimental deposition time). Thin films containing the nanomaterials were prepared by placing the composite mate-

(24) Zalusky, A. S.; Olayo-Valles, R.; Wolf, J. H.; Hillmyer, M. A. *J. Am. Chem. Soc.* **2002**, *124*, 12761−12773.
(25) Wolf, J. H.; Hillmyer, M. A. *Langmuir* **2003**, *19*, 6553−6560.
(26) The nanoporous polymer monoliths have typical pore sizes of 20−50 nm and pore volumes of ca. 0.5 mL/g.
(27) Malinauskas, A. *Polymer* **2001**, *42*, 3957−3972.
(28) Murray, C. B.; Norris, D. J.; Bawendi, M. G. *J. Am. Chem. Soc.* **1993**, *115*, 8706−8715.

Table 1. Nanoporous Polymers Used for Template Syntheses

sample	M_n (kg/mol) PCHE or PS[a]	M_n (kg/mol) PLA[b]	M_w/M_n[c]	f_{PLA}[d]	r[e] (nm)	V[f] (mL/g)
PCHE1	5.2	5.1	1.17	0.43	6.3	0.77
PCHE2	25	13	1.11	0.28	9.8	0.43
PCHE3	25	14	1.14	0.30	12.9	0.47
PCHE4	25	19	1.14	0.37	15.4	0.61
PCHE5	42	26	1.11	0.32	24.0	0.50
PS1	20	15	1.07	0.36	11.2	0.54
PS2	34	24	1.10	0.38	15.5	0.59
PS3	56	36	1.16	0.36	22.5	0.54

[a] The number average molecular weights of PS and PCHE were determined from ^{1}H NMR spectroscopy. [b] Number average molecular weight of PLA in the corresponding precursor was determined from ^{1}H NMR spectroscopy. [c] SEC of the diblock precursors versus polystyrene standards. [d] Volume fraction of PLA calculated using the following densities $\rho_{PS} = 1.02$ g/cm^3 and $\rho_{PLA} = 1.18$ (at 110 °C); $\rho_{PCHE} = 0.849$ g/cm^3 and $\rho_{PLA} = 1.114$ g/cm^3 (at 187 °C).[33,34] [e] Cylinder radius calculated from the SAXS principal peak position at RT and f_{PLA}. [f] Estimated pore volume $= 2\pi r^2/(\sqrt{3}a^2 f_{PS(PCHE)}\rho_{PS(PCHE)})$, using $\rho_{PCHE} = 0.947$ g/cm^3 at RT[35] and $\rho_{PS} = 1.04$ g/cm^3 at RT.

rial in THF or toluene at approximate concentrations of 0.5 wt % to dissolve the template. The solutions were either spin-coated at a rate of 2000 rpm or simply cast onto brass SEM shims or carbon-coated TEM grids (Ted Pella). TEM analysis was performed on either uncoated thin films or microtomed sections of material using a JEOL 1210 TEM operating at 120 kV. Microtoming of the TEM samples was performed on a Reichert Cryo-Ultramicrotome using a diamond knife at room temperature.

Materials. Commercial solvents and reagents were used as-received except as noted. *N*,*N*-Dimethylformamide (DMF) was stored over molecular sieves and purified THF was obtained by passage through an activated alumina column to remove protic impurities using a home-built purification system.[29] Pyrrole (Aldrich, 98%), ferric chloride (Fischer, certified A.C.S. lump), cadmium acetate dihydrate (Aldrich, 98%), sodium sulfide nonahydrate (Aldrich, 98%), benzenethiol (Aldrich, 98%), sulfur (Aldrich, sublimed), and thiourea (Aldrich, 99%) were used without further purification.

Template Materials. The nanoporous PS and PCHE monoliths used as templates were prepared from PS−PLA and PCHE−PLA diblock copolymer precursors as described previously.[23−25] Briefly, diblock copolymers of PS−PLA or PCHE−PLA were synthesized by anionic polymerization of styrene followed by end functionalization with ethylene oxide to produce hydroxyl-terminated polystyrene (PSOH). To form hydroxyl-terminated polycyclohexylethylene (PCHEOH), the PSOH precursor was hydrogenated over Pd on $CaCO_3$ at 500 psig H_2 and 120 °C. Following the synthesis of the first block, the second block was synthesized by ring-opening polymerization of D,L-lactide to form diblock copolymers with PLA as the cylindrical minor component in a matrix of PS or PCHE. The polymer samples were channel die-processed to align the PLA cylinders along the direction of polymer flow within the channel die at 125 °C for PS−PLA and 175 °C for PCHE−PLA. Channel die-aligned monolithic pieces (typically 55 × 2 × 1 mm) were then fractured into smaller monoliths (typically 4 × 2 × 1 mm) and placed into a 0.5 M solution of NaOH in 60:40 H_2O:MeOH at 65 °C for 1 week. This treatment resulted in the degradation of the PLA cylinders, leaving behind a nanoporous monolith of PS or PCHE. The nanoporous polymer monoliths were then dried in a vacuum oven at room temperature for 16 h. See Table 1 for a summary of the molecular parameters for each of the polymer templates.

Solution Polymerization of Pyrrole.[30] Pyrrole (2.20 g, 0.033 mol) was added to 150 mL of distilled water. $FeCl_3 \cdot 6H_2O$ (19.4 g, 0.072 mol) was dissolved in 150 mL of distilled water to make a clear orange solution. The two mixtures were combined and stirring was begun. Within a minute, the solution turned black and opaque. After 24 h, a black precipitate was isolated by vacuum filtration and washed with water and methanol until the filtrate was colorless. The product was dried under vacuum at 60 °C for 12 h. The mass of polymer recovered was 2.11 g (96%).

Table 2. Summary of PPY Filling of Nanoporous PCHE Monoliths

entry	template (pore diameter/nm)	PCHE (mg)	PPY[a] (mg)	time (h)	% filling[b]
1	**PCHE4**(31)	7.4	0.3	1.75	4.5
2	**PCHE4**(31)	6.7	0.7	16.5	12
3	**PCHE4**(31)	6.9	1.2	40.5	19
4	**PCHE4**(31)	8.2	1.7	92.5	23
5	**PCHE4**(31)	9.5	4.2	192	50
6	**PCHE2**(19)	10.1	1.0	132	16
7	**PCHE5**(48)	10.8	2.2	144	28

[a] Mass of PPY formed within the PCHE template (does not include mass of $FeCl_3$). [b] Calculated from the pore volume of PCHE (see Table 1) and the reported density of PPY, 1.47 g/mL.[31]

Fe(III) Oxidant Loading. The iron oxidant used in the polymerization of pyrrole was deposited into the pores of a PCHE template from a methanol solution. A typical loading procedure was as follows. A 0.65 M solution of Fe^{3+} was prepared by dissolving 0.7 g of $FeCl_3 \cdot 6H_2O$ in 4.0 mL of methanol. An 8.2-mg sample of nanoporous **PCHE4** in Table 1 was soaked in the Fe^{3+} solution for 12 h. After removal from the oxidant solution, the outside of the monolith was washed generously with methanol to remove excess salt. The oxidant-filled monolith was dried under vacuum for 12 h at room temperature. The previously white monolith was rusty orange in color throughout the piece. The nanoporous material used here had an estimated pore volume of 0.61 mL/g (see Table 1). This corresponded to a total pore volume of 5.0×10^{-3} mL for the 8.2-mg sample. On the basis of the concentration of the iron solution (0.10 g/mL), the expected mass of $FeCl_3$ to be deposited was 0.5 mg. The experimental mass gain was 0.2 mg, 40% of the expected value.

Template Synthesis of Polypyrrole Nanomaterials. PPY was synthesized within the nanoporous PCHE template by placing the oxidant-loaded monolith into a small vial, which was sealed in a chamber saturated with pyrrole vapors. The Fe^{3+}-loaded monoliths were placed into open vials that were enclosed in a large glass container containing liquid pyrrole. The monoliths were protected from the liquid by the smaller vials, but were exposed to the pyrrole vapor through the vial openings. Within 30 s, the edges of the PCHE piece containing open pores changed from orange to black in color, indicating the presence of PPY. Within 2 min the outside of the entire piece appeared black. The 8.2-mg PCHE monolith described above was exposed to pyrrole vapors for 92.5 h. Considering the pore volume of 5.0×10^{-3} mL for this sample and the room-temperature density of PPY of 1.47 g/mL,[31] the expected mass increase for complete PPY filling was 7.4 mg. Experimentally, 1.7 mg of PPY was formed within the template, corresponding to 23.1% filling after 92.5 h. The degree of filling of the PCHE template was dependent on the reaction time and ranged from 4.5% filling for a polymerization time of 1.75 h to 49.3% filling after 144 h (see Table 2). The PCHE template was removed from the PPY nanomaterials with THF, a good solvent for PCHE and a nonsolvent for PPY.

Cd(II) Loading. Cd^{2+} was adsorbed within the pores of a nanoporous PS monolith by means of a methanol solution of cadmium acetate. A typical preparation was as follows. A 2.5 M solution of $Cd(OAc)_2 \cdot 2H_2O$ was prepared by dissolving 6.66 g (0.025 mol) in 10 mL of methanol. A PS monolith (14.6 mg) was soaked in the solution of cadmium acetate for 24 h. The monolith was removed from the solution, washed with copious

(29) Schmidt, S. C.; Hillmyer, M. A. *Macromolecules* **1999**, *32*, 4794−4801.
(30) Martin, C. R. *Chem. Mater.* **1996**, *8*, 1739−1746.
(31) Geiss, R. H.; Street, G. B.; Volksen, W.; Economy, J. *IBM J. Res. Dev.* **1983**, *27*, 321−329.

Table 3. Degree of Pore Filling with CdS Particles in Nanoporous PS Monoliths

template (method)	pore volume[a] (μL)	mass of CdS (mg)	volume of CdS[b] (mL × 10^{-4})	% pore volume filled
PS1(1)	5.8	1.0	2.1	3.6
PS1(1)	6.6	4.2	8.7	13
PS1(1)	3.6	0.7	1.4	3.9
PS1(2)	8.9	5.6	12	13
PS1(3)	16.7	9.0	19	11

[a] Based on the calculated pore volume of nanoporous PS monoliths (see Table 1) and the mass of sample used. [b] Based on the density of bulk CdS, 4.82 g/mL.

amounts of H_2O to remove any excess Cd^{2+} present on the outer surface of the monolith, and dried in air overnight. The mass of the PS/Cd^{2+}monolith was 16.0 mg, which corresponded to 8.8% pore filling by volume.

PS/CdS Nanoporous Monoliths. CdS was synthesized within nanoporous PS monoliths by reaction of the Cd^{2+} ions adsorbed onto the PS monolith with S^{2-} anions in solution. Three different methods were used. Representative syntheses for each method are presented below. Table 3 shows a summary of the amount of pore filling for each of the three methods.

Method 1. A PS monolith (10.7 mg) was impregnated with Cd^{2+} as described above. The Cd^{2+}-soaked monolith was then soaked in a solution of 1.67 M $Na_2S{\cdot}9H_2O$ (53:47 H_2O:MeOH). Within 30 s the monolith appeared completely yellow. The reaction was allowed to continue for 24 h before the monolith was removed and washed with H_2O and MeOH. The mass of the composite PS/CdS monolith was 11.7 mg.

Method 2. A PS monolith (16.5 mg) was impregnated with Cd^{2+} as described above. The Cd^{2+}-soaked monolith was then soaked in a 0.5 M solution (50:50 MeOH:H_2O) of thiourea (pH adjusted to 9−11 with NH_3) and heated to 75 °C. Thiourea releases S^{2-} at high pH (9−11) and elevated temperature (>60 °C)[32] and reacts very quickly with Cd^{2+} to form CdS. After being heated for 15 min, the monolith appeared yellow. Heating was continued for 30 min before the monolith was removed and washed with H_2O and MeOH. The mass of the composite PS/CdS monolith was 22.1 mg.

Method 3: Capping Reagent. A PS monolith (31.0 mg) was impregnated with Cd^{2+} as described above. Under an inert atmosphere of Ar the Cd^{2+}-impregnated PS monolith was soaked in a methanol solution of 0.1 M $Na_2S{\cdot}9H_2O$ and 0.2 M benzenethiol. The monolith began to turn yellow almost immediately and within 30 s was completely yellow. After 24 h, the monolith was removed and washed with H_2O and MeOH. The mass of the composite PS/CdS-benzenethiol monolith was 40.0 mg.

Results and Discussion

Synthesis of Nanoporous Polymer Monoliths. Nanoporous polymer monoliths were synthesized from diblock copolymers containing a degradable segment. The diblock copolymers were synthesized such that the degradable component formed cylinders in a matrix of a nondegradable polymer. Specifically, we synthesized polystyrene-*block*-polylactide (PS−PLA)[23,24] and polycyclohexylethylene-*block*-polylactide (PCHE-PLA)[25] with appropriate PLA volume fractions to obtain a cylindrical morphology. The PLA cylinders were aligned through channel die processing. The cylinders aligned parallel to the direction of polymer flow within the channel die. Treatment of the monoliths with a solution of NaOH in water/methanol at 65 °C for 1 week degraded the PLA cylinders while leaving the PS or PCHE matrix intact. The resulting monolithic material consisted of a PS or PCHE framework containing a hexagonally packed arrangement of nanopores. The nature of the matrix in terms of its chemical and thermal stability influences the strategies available for template synthesis. PCHE is more solvent-resistant and is more thermally stable than PS. The preparation of polypyrrole nanowires described hereafter required the use of nanoporous PCHE materials since the integrity of the PS framework was compromised in the presence of pyrrole vapor whereas the methods employed in the synthesis of CdS nanoparticles leave the PS matrix unharmed. The characteristics of the nanoporous polymer templates used are summarized in Table 1.

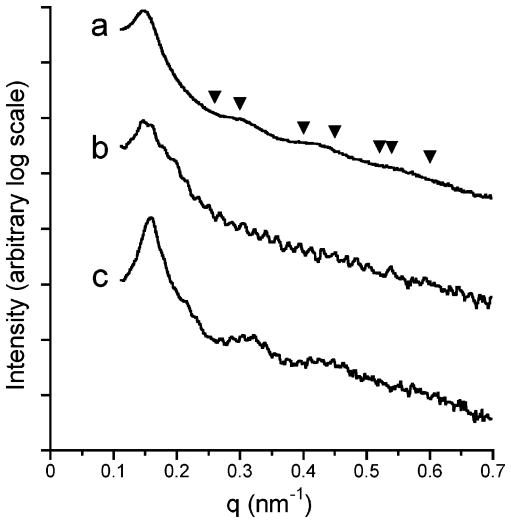

Figure 2. 1D SAXS patterns of (a) nanoporous **PCHE4** in Table 1, (b) **PCHE4** after loading with $FeCl_3$, and (c) **PCHE4**/PPY showing that the ordered framework was retained through these processes. ▼ at $\sqrt{3}q^*$, $\sqrt{4}q^*$, $\sqrt{7}q^*$, $\sqrt{9}q^*$, $\sqrt{12}q^*$, $\sqrt{13}q^*$, and $\sqrt{16}q^*$ are characteristic of a cylindrical morphology (q^* is the principal peak).

Template Synthesis of Polypyrrole Nanowires. The template synthesis of PPY was performed within nanoporous PCHE by exposing an oxidant-loaded monolith to pyrrole vapors. The Fe^{3+} oxidant was deposited into the nanoporous PCHE from a methanol solution of $FeCl_3$. After drying, the monoliths had increased in mass, but only 40% of the expected value based on the estimated pore volume of the nanoporous PCHE and the concentration of the $FeCl_3$ solution. This discrepancy could be due to loss of Fe^{3+} during washing, pore blockage, or an overestimation of the pore volume given in Table 1. Despite the fact that the Fe^{3+} loading was lower than expected, the orange color of the iron salt was observed throughout the piece when fractured. Small-angle X-ray scattering (SAXS) of the material post $FeCl_3$ impregnation verified the preservation of the framework (Figure 2).

The Fe^{3+}-loaded monoliths were then exposed to the pyrrole vapor and within 30 s the ends of the monoliths (presumably containing ended cylinders) began to turn black, indicating the formation of PPY. After several minutes the entire piece appeared black and the fractured surface of this PCHE monolith was also black (Figure S1). The amount of PPY deposited into the PCHE template increased with exposure time to the pyrrole vapor. The first five entries of Table 2 show the

(32) Abd-Lefdil, S.; Messaoudi, C.; Abd-Lefdil, M.; Sayah, D. *Phys. Status Solidi A* **1998**, *168*, 417−423.

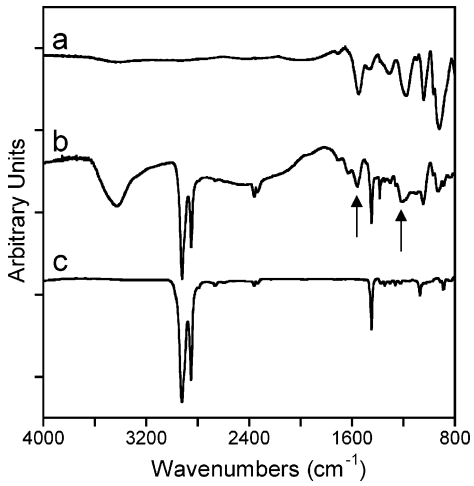

Figure 3. IR spectra of (a) PCHEOH, (b) **PCHE4**/PPY composite material, and (c) PPY. The arrows mark the peaks at 1548 and 1180 cm^{-1} in the composite material due to the presence of PPY in the sample. The broad peak at 3430 cm^{-1} in (b) is attributed to residual water in the KBr used to prepare the sample.

results of an experiment where a set of PCHE monoliths were exposed to pyrrole vapors for different lengths of time. The longest reaction time resulted in the most PPY filling, ca. 50%, based on calculated pore volume (Table 1).

While we expected the amount of filling to increase with time, consumption of the oxidant should limit the PPY mass. However, the amount of PPY formed in all cases exceeded the expected amount given the level of Fe^{3+} present in the monolith. For example, for the fourth entry in Table 2, 0.2 mg of $FeCl_3$ (1.2×10^{-6} mol) was deposited. Because the Fe^{3+} is expected to dope the polymer chain as it is synthesized and activate the monomers for polymerization, 2.25 mol of Fe^{3+} should be consumed for each mole of monomer incorporated into the polymer.[36] Therefore, we expected that 5.3×10^{-7} mol (0.04 mg) of pyrrole would be polymerized, but 1.7 mg of PPY was formed. In the experiments performed on the benchtop, over the course of the reaction, the Fe^{3+} was possibly regenerated through air oxidation of the Fe^{2+} product.[37] Inaccuracies in the mass measurements or dissolution of monomeric pyrrole in the PCHE matrix are other possible reasons for this discrepancy. However, the latter is unlikely given the low-solubility parameter of PCHE.[25]

The presence of PPY in the composite material was confirmed by infrared spectroscopy (Figure 3). The spectrum of PCHE/PPY composite contains PCHE peaks at 2921 and 2849 cm^{-1} and several characteristic PPY peaks including those at 1548 and 1180 cm^{-1}. The composite material displayed a broad peak at 3430 cm^{-1} that we attribute to water in the potassium bromide used to prepare the sample.[38] After PPY was incorporated into the monolith, the morphological structure of the composite was analyzed by SAXS (Figure 2). SAXS showed that the structure of **PCHE4** remained intact after the 192-h polymerization of pyrrole confirming retention of the original topology. To obtain real-space images of the PPY in the template, we immersed a portion of the composite in THF. The insolubility of PPY and the solubility of PCHE in THF allowed for the removal of the PCHE template through dissolution without affecting the PPY nanomaterials. SEM analysis after treatment with the solvent revealed an arrangement of individual PPY nanowires protruding from the PCHE template surface (Figure 4a). The exposed PPY nanowires have a diameter of 30 nm, consistent with the pore dimensions. In addition, the nanowires showed the same preferred direction (shear flow direction) as the nanopores of the PCHE template.

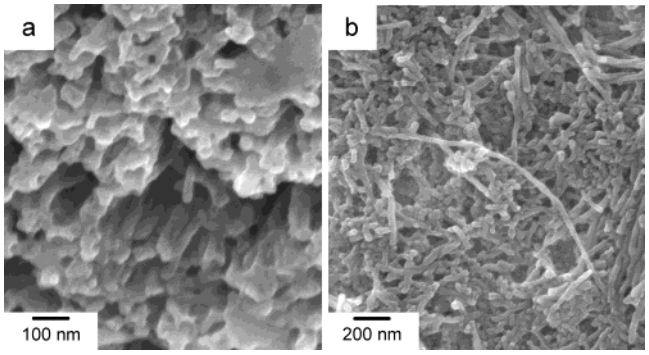

Figure 4. SEM image of (a) PPY-filled **PCHE4** where the template has been dissolved from the surface to reveal PPY wires and (b) an agglomeration of PPY nanowires from a spin-coated solution of **PCHE4**/PPY.

The PCHE template was then completely removed by dissolution in THF to form a 0.5 wt % mixture, which was then spin-coated onto a brass shim for SEM analysis. Black particulates were observed in the mixture as the PCHE template dissolved, presumably due to aggregation of the PPY nanomaterials. Nanowire agglomeration could have resulted from the high surface energy of the PPY nanomaterials and their dislike for THF. Figure 4b shows an SEM image of a collection of templated PPY nanowires from a spun-cast sample. As with the partially dissolved composite material (Figure 4a), the nanowires exhibited diameters that matched the template dimensions. While difficult to distinguish the length of the nanowires due to their agglomeration and arrangement, the longest single PPY nanowire observed had a length of 1.6 μm and an aspect ratio of ca. 46.

Figure 5 shows a TEM micrograph of a spin-coated sample of PPY nanowires from **PCHE4**/PPY onto a carbon-coated Cu TEM grid. This image shows a more

(33) Zhao, J.; Hahn, S. F.; Hucul, D. A.; Meunier, D. M. *Macromolecules* **2001**, *34*, 1737−1741.
(34) Witzke, D. R.; Narayan, R.; Kolstad, J. J. *Macromolecules* **1997**, *30*, 7075−7085.
(35) Hucul, D. A.; Hahn, S. F. *Adv. Mater.* **2000**, *12*, 1855−1858.
(36) Walker, J. A.; Warren, L. F.; Witucki, E. F. *J. Polym. Sci., Part A: Polym. Chem.* **1988**, *26*, 1285−1294.
(37) An additional PPY filling experiment was performed on a 13.2-mg PCHE monolith loaded with 0.4 mg of oxidant as above, except that it was assembled in an argon atmosphere of a drybox. The system was sealed and left in the drybox for 166 h. During this time, the PCHE monolith turned black as expected, but showed only 11% filling. The mass of PPY formed, 1.3 mg, was still greater than the expected 0.07 mg, based on the amount of oxidant present, but the degree of filling in this case was much less than that of a comparable experiment performed in air. In the drybox experiment there could have still been oxidation of the Fe^{2+} product by species in the unpurified pyrrole or trace amounts of oxygen in the controlled environment.
(38) PCHE4/PPY was analyzed by ^{13}C solid state NMR. The spectrum contained a distinct peak at 116 ppm which we attribute PPY. The peak is well above those expected for PCHE and is consistent with previously reported ^{13}C solid-state NMR data for PPY. See Forsyth, M.; Truong, V.-T.; Smith, M. E. *Polymer* **1994**, *35*, 1593−1601.

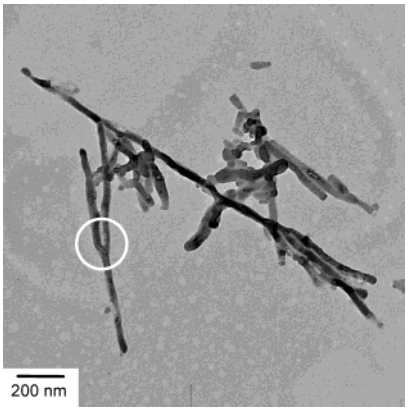

Figure 5. TEM image of a spin-coated solution of **PCHE4**/PPY. The circle highlights a branch point in a PPY nanowire.

dispersed set of wires relative to the SEM images. Solid nanowires with diameters ca. 30 nm of varying lengths are evident in this image with the longest contiguous wire observed being almost 2 μm.[39] In theory, it would be possible to synthesize much longer wires using the monolithic PCHE templates, but the spin-coating process could be damaging to the PPY nanowires. This image also allowed for the observation of another interesting feature not readily apparent in the SEM images. Many branch points are present in the PPY structures. Branch points in the nanowires are the product of defects in the nanoporous structure of the PCHE template. Defects in which two channels merge into one have been observed in this type of nanoporous material.[24] The branch defects add to the problem of nanowire agglomeration as the templated materials are presumably interconnected.

The ability to modify the pore size in the template through synthetic methods allowed for the preparation of PPY nanowires of varying diameter. PPY nanowires were prepared in two other templates (**PCHE2** and **PCHE5** in Table 2) containing different pore diameters. As before, complete filling was not obtained but still exceeded that expected given the amount of Fe^{3+} loaded into the monoliths. After vapor-phase polymerization of pyrrole in the voids, the composites were dissolved and the solutions were cast onto carbon-coated copper grids and analyzed by TEM (Figure 6). Comparison of the images indicated an ability to tune the nanomaterial diameter by using the different monolithic nanoporous templates.

Template Synthesis of Nanoscopic CdS. The nanoporous monolithic templates were also used as hosts for the preparation of an inorganic nanomaterial, CdS. In this protocol, the synthetic methods employed allowed for the use of nanoporous PS monoliths. The template synthesis of CdS was performed in a two-step process. In the first step, Cd^{2+} ions were adsorbed onto the pore surface from a concentrated solution of cadmium acetate dihydrate in methanol. This step was performed in a manner similar to the adsorption of Fe^{3+} described previously and the adsorption results were similar. After soaking for a period of 24 h, the monolith was removed from solution, washed with water, and dried. Using the mass increase, the pore volume of the monolith, and the density of $Cd(OAc)_2$, the amount of filling with cadmium acetate was calculated. It was found that the amount of filling was ca. 9% (4% Cd^{2+}) of the pore volume for **PS1** in Table 2. This value was ca. 30% of the expected based on the concentration of the cadmium acetate solution and the estimated pore volume. Like the adsorption of Fe^{3+} discussed previously, the lower than expected filling may be the result of ion loss during the washing step, a sieving mechanism whereby the concentration of the solution is not reflected within the pores of the PS monolith or errors in the mass measurements of small quantities. The loading of the Cd^{2+} was followed by exposure to a sulfur source, either sodium sulfide or thiourea (see Experimental Section). The nanoporous PS monoliths turned uniformly yellow, indicating the presence of CdS within the templates. Fracturing of the monoliths perpendicular to the channel direction revealed that the monoliths were yellow throughout. Longer reaction times did not increase the amount of CdS produced as it did with PPY; the amount of CdS synthesized was limited by the amount of Cd^{2+} deposited onto the pore surface. The amount of pore filling is summarized in Table 3 for the different methods.

To determine if the growth of particles within the PS was affecting the ordered structure of the porous template, SAXS patterns obtained before and after growth of CdS were compared (Figure 7). We observed that the cylindrical morphology of the template was retained after the incorporation of CdS into the framework. In an attempt to provide real-space images of the composite materials, SEM micrographs were obtained. Unfortunately, we did not observe areas containing particles of higher atomic number, despite the composite material being uniformly yellow across the fracture surface (Figure S2). The failure to observe the particles by SEM could be the result of the limited CdS loading within the nanoporous PS monolith or the small area and depth surveyed. However, the SEM images confirmed the SAXS results, showing that the cylindrical morphology was maintained throughout the templating process.

As with the preparation of PPY nanowires, the ability to control the size of the CdS nanoparticles through the use of different templates was explored (**PS1**−**PS3**, Table 1). To elucidate whether the size of the CdS nanoparticles was being controlled by the pore diameter of the template, the composite materials were analyzed by WAXS (Figure 8). The CdS-impregnated PS monoliths showed broad peaks at 26.5, 44.1, and 51.6° 2θ, indicating the presence of the wurtzite structure of CdS (compared to PDF# 41-1049) within the pores. The sizes of the CdS particles were estimated from the peak broadening in the WAXS spectra by employing the Scherrer equation.[40] The estimated diameters of the CdS particles matched well with the channel dimensions of each of the PS templates employed (Table 4). This result shows that the size of the growing CdS particles

(39) PPY templating experiments using nanoporous membranes and liquid-phase polymerization of pyrrole have demonstrated that at long reaction times solid PPY nanowires were formed, while at shorter reaction times hollow nanowires or "nanotubules" resulted. Under the vapor-phase polymerization conditions utilized here, this phenomenon was not observed.

(40) Cullity, B. D. *Elements of X-ray Diffraction*, 2nd ed.; Addison-Wesley Publishing Company, Inc.: Reading, MA, 1978.

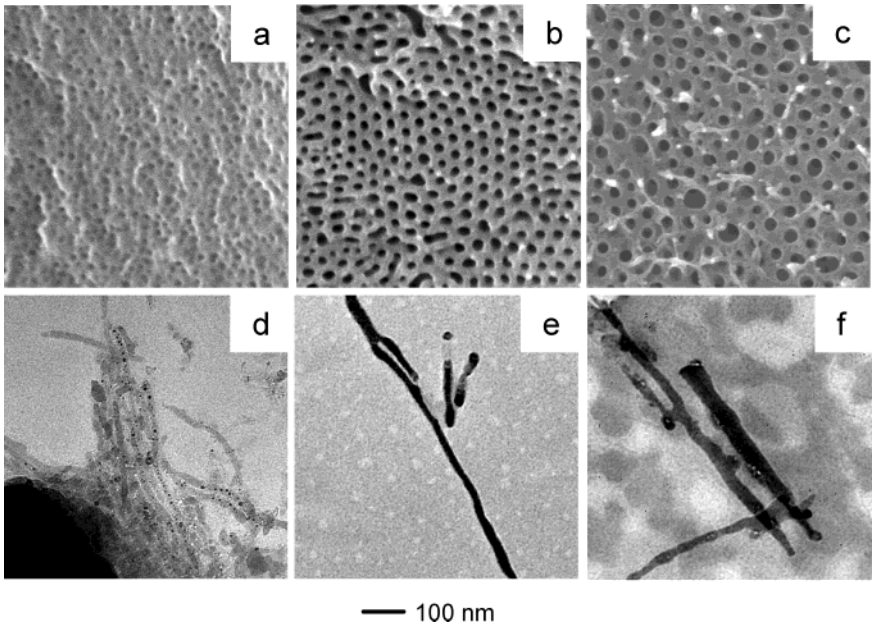

Figure 6. SEM images of nanoporous PCHE templates: (a) **PCHE2**, (b) **PCHE4**, and (c) **PCHE5**. TEM images of PPY nanowires templated from (d) **PCHE2**, (e) **PCHE4**, and (f) **PCHE5** displaying control of nanowire diameter. Images (a) and (d), 19-nm template and wire; images (b) and (e), 31-nm template and wire; images (c) and (f), 48-nm template and wire.

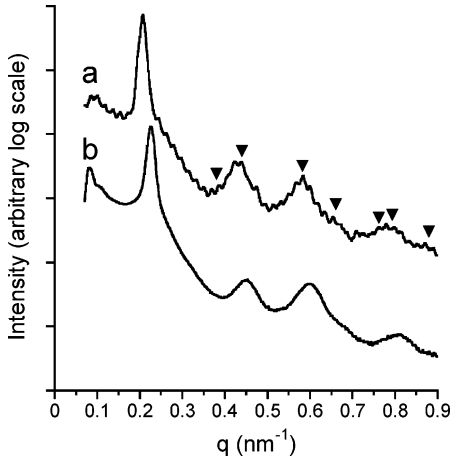

Figure 7. 1D SAXS patterns for a (a) nanoporous PS monolith, **PS1** in Table 1, and (b) nanoporous PS monolith/CdS composite material. Nanoscopic order remains after growth of CdS within the PS hosts pores. ▼ at $\sqrt{3}q^*$, $\sqrt{4}q^*$, $\sqrt{7}q^*$, $\sqrt{9}q^*$, $\sqrt{12}q^*$, $\sqrt{13}q^*$, and $\sqrt{16}q^*$ are characteristic of a cylindrical morphology (q^* is the principal peak).

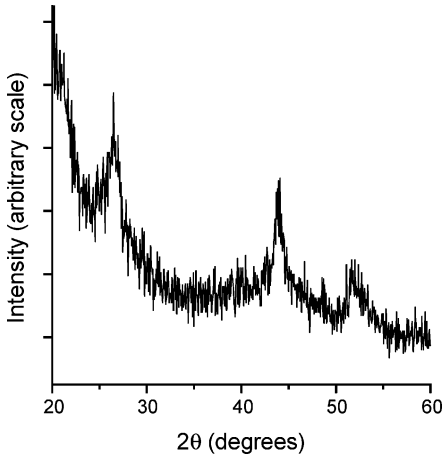

Figure 8. Typical WAXS pattern for a nanoporous PS monolith/CdS composite material showing the diffraction peaks for the hexagonal (wurtzite) structure of CdS at 26.5, 44.1, and 51.6° 2θ.

is being restricted by the pores of the PS matrix as it was for the PPY nanowires.

To further study the size and morphology of the CdS particles templated by the porous frameworks, TEM images of the resultant materials were acquired. Microtomed thin sections (ca. 50-nm thickness) of the PS/CdS composites were obtained from the center of the material. These sections allowed for the visualization of CdS particles still held within the PS template. Figure 9 shows TEM micrographs of the microtomed sections obtained from the three PS hosts of differing pore diameter. The images revealed that the majority of the CdS particles were spherical, with a few elongated particles evident in the templates with 31- and 44-nm pore diameters. Analysis of the images confirmed that the sizes of the CdS particles confined within the pores of the porous template agreed with the channel dimensions and also the estimations made from the WAXS analysis (Table 4). The spherical nature of the particles indicated that the CdS grew as small, isolated islands, rather than uniformly across the pore surface. This result was expected because the adsorbed Cd^{2+} was in relatively low concentration compared to the pore volume and not all pore walls would be fully covered. The

Table 4. Control of the CdS Particle Size with Nanoporous PS Pore Size

trial	template	average template pore diameter (nm)	CdS synthesis method[a]	average particle diameter (WAXS)[b] (nm)	average particle diameter (TEM) (nm)
1	**PS1**	22	1	19	n/a
2	**PS1**	22	2	20	20 ± 5
3	**PS2**	31	1	29	27 ± 5
4	**PS3**	45	1	48	43 ± 10

[a] See Experimental Section. [b] Scherrer equation, $t = 0.94\lambda/B \cos\theta$, where B is the line broadening in radians, θ is the Bragg angle, and $\lambda = 1.542$ Å (Cu Kα).

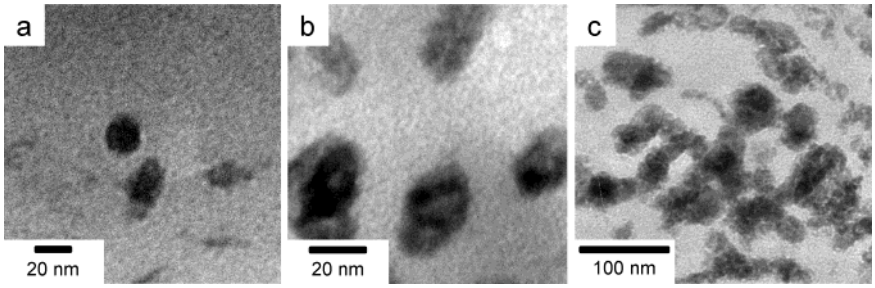

Figure 9. TEM micrographs of microtomed sections of PS/CdS composite material showing control of the CdS particle size using PS templates: (a) **PS1** (22-nm pore diameter), (b) **PS2** (31-nm pore diameter), and (c) **PS3** (45-nm pore size template) in Table 1.

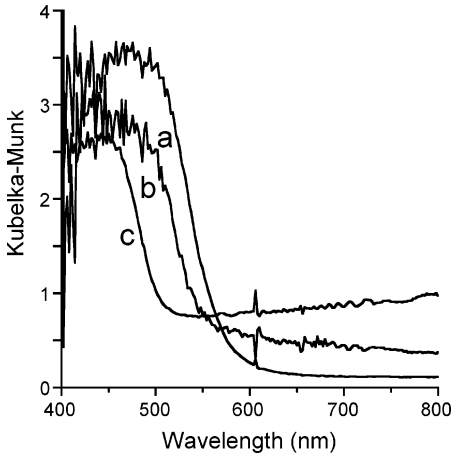

Figure 10. DR−UV−Vis spectra comparing (a) bulk CdS, (b) PS monolith/CdS composite, and (c) PS monolith/CdS−benzenthiol composite. The band edge in (c) has blue-shifted ca. 30 nm.

CdS particles also appeared to be distributed randomly within the microtomed sections rather than in straight lines as might be expected if the particles were lined up within a template channel. This lack of order may be the result of the imperfect alignment of the pores in the template material, observing many layers of CdS particles simultaneously, or because alignment of the pore channels was compromised during microtoming.

In an effort to obtain particle sizes smaller than the templates available but still incorporate them into the nanoporous polymer host, our original CdS synthesis was modified. A ligand "capping" agent (benzenethiol) was added to the sulfur solution which restricted the growth of the CdS particles by replacing surface sulfur atoms with benzenethiol groups. The synthesis progressed much like the synthesis of CdS grown without capping agent within the PS host. After a few minutes the PS monolith had turned uniformly yellow; the reaction was continued for 24 h. CdS particles grown in this manner were smaller than the pore diameters and showed a quantum size effect (QSE). This was evident when comparing the diffuse reflectance UV−Vis (DR−UV−Vis) spectra of bulk CdS, nanoporous PS/CdS monoliths, and nanoporous PS/CdS-benzenthiol monoliths (Figure 10). The CdS synthesized within the PS matrix without benzenethiol has a band edge consistent with bulk CdS; that is, it had the electronic properties of bulk CdS and showed no QSE. The CdS synthesized in the presence of benzenethiol capping agents, however, shows a slight QSE. The band edge is blue-shifted ca. 30 nm from 512 nm (bulk) to 484 nm.

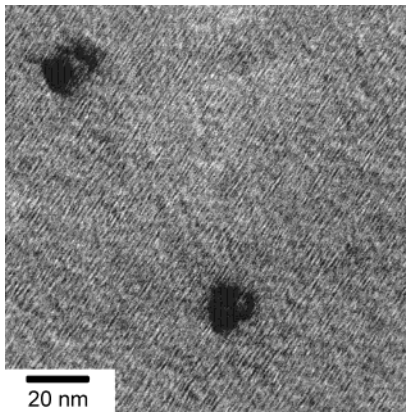

Figure 11. TEM micrograph of a spun-cast solution of CdS nanoparticles capped with benzenethiol.

Using the shift in band edge, it is possible to calculate the size of the CdS nanoparticles, which yielded a nanoparticle diameter of 6.8 nm.[41] To further examine the size of the nanoparticles, the polymer host was removed by dissolution in toluene and a spun-cast sample was analyzed by TEM (Figure 11). The images showed that the CdS nanoparticles were on the order of 10 nm in diameter compared to a template pore diameter of 22 nm. Little aggregation between particles was observed. Whereas, in spun-cast solutions of CdS particles prepared with no capping agent, the particles agglomerated (Figure S3). The dispersion of individual nanoparticles prepared with the capping agent is presumably due to the presence of surface phenyl groups, which inhibit aggregation. This preparative method combines both physical and chemical growth restriction methods. The chemical agent, benzenethiol, limited the size of the nanoparticles which as a result showed a QSE while the host restricted the growth to a specific area.

Conclusion

Nanoporous PS and PCHE monoliths prepared from diblock copolymer precursors were successfully used as templates for the synthesis of PPY nanowires and nanoscopic CdS particles. The methods employed in the syntheses resulted in intact nanoporous polymer monoliths that retained their morphology after incorporation of the nanomaterials into the framework. The PPY nanowires and CdS nanoparticles were shown to have dimensions that corresponded to the size of the nan-

(41) Banerjee, R.; Jayakrishnan, R.; Ayyub, P. *J. Phys.: Condens. Matter* **2000**, *12*, 10647−10654.

oporous structure. The feature size of either the nanowires or nanoparticles was tunable by using nanoporous monoliths containing different pore dimensions. The size of the CdS nanoparticles was also controlled through a synthetic method that chemically restricted the growth of the particles. In addition to the synthesis of discrete nanomaterials, the template synthesis techniques discussed here may be useful for the preparation of novel composite materials incorporating nanostructure semiconductors or conducting polymers in an insulating polymer matrix.

Acknowledgment. This research was supported by the Industrial Partnership for Research in Interfacial and Materials Engineering (IPrime) at the University of Minnesota, the National Science Foundation (DMR-0094144), and the David and Lucile Packard Foundation. This work was also supported in part by the MRSEC Program of the National Science Foundation under Award Number DMR-0212302. We thank Professor Michael D. Ward for helpful discussions.

Supporting Information Available: Figures S1, S2, and S3 (PDF). This material is available free of charge via the Internet at http://pubs.acs.org.

CM0350075